ELSEVIER

Chemical Engineering Journal 72 (1999) 97–107

Chemical Engineering Journal

Turbulence characteristics in turbine-agitated tanks of different sizes and geometries

Eva Ståhl Wernersson, Christian Trägårdh*

Food Engineering, Lund University, PO Box 124, S-221 00, Lund, Sweden

Received 30 March 1998; received in revised form 7 October 1998; accepted 22 October 1998

Abstract

Velocity measurements have been conducted with constant temperature anemometry in three reactors, with diameters of 0.8, 1.88 and 2.09 m. Their impeller-to-tank-diameter ratios were 3, 2.47 and 3, and they were equipped with two three and four Rushton turbines. Turbulence parameters, intensity, turbulent kinetic energy, local energy dissipation rate and energy spectra, were calculated from the measured data. The turbulent kinetic energy was constant in the local flow situation, when scaled with the square of the convective velocity. This was independent of position, agitation rate and size of reactor, in the impeller zone. The energy spectra in the impeller zone were almost constant when scaled with the local energy dissipation length, independent of position, agitation rate and size of reactor. The local energy dissipation rate scaled with the cube of the convective velocity and impeller diameter.

Keywords: Anemometry measurements; Geometry; Turbulent kinetic energy

1. Introduction

Turbulence characteristics are of interest for the scale-up of a reactor, since they affect the general mixing performance as well as the mass transfer properties of a reactor. The objective of this study was to compare the turbulence characteristics of a tank of pilot size (diameter 0.8 m), with those of two industrial reactors of different sizes and geometries and under operating conditions in use in industrial practice during fermentation.

Several studies on turbulence characteristics in turbine-agitated tanks have been presented in the literature, but most of the measurements have been conducted in small tanks of bench scale, $D_{tank} \leq 0.30$ m, [1–9]. To our knowledge, no liquid turbulence measurements have been made in industrial reactors of the size as in this study, but some have been carried out in pilot-sized units as seen below.

Local turbulent parameters are often scaled with a modified impeller tip speed, nd_{imp}, or impeller tip speed, v_{tip}, and in earlier measurements presented by Ito [10], the turbulence intensity used this scaling. They used a measuring method based on an electrochemical reaction to measure the mass transfer, by a multi-electrode probe. However, Ito et al. carried out their experiments in a small tank ($D_{tank} = 0.3$ m). Coustes and Couderc [11] used laser Doppler anemometry (LDA) measurements in two reactors of similar geometry, but with different sizes. Mean velocities and velocity fluctuations were measured at two agitator rates in the smaller tank and at one agitation rate in the larger tank. They stated that the dimensionless profiles of these parameters were independent of agitation rate and their measurements scaled with nd_{imp}. In our previous measurements [12], neither the mean velocity nor the turbulent intensity scaled with v_{tip} to a constant value.

Nishikawa [13] used CTA measurements to compare three geometrically similar reactors with tank diameters of 0.15 m, 0.30 m and 0.90 m. They concluded that energy spectra could be scaled by the energy dissipation length, λ_f, for measurements at geometrically similar positions. Kolmogorov's length, l_K, and velocity, v_K scales were also used as scaling factors, but since the spectra resulted in wavenumbers smaller than $1/l_K$, they do not scale the spectra.

Van der Molen and van Maanen [14], measured turbulence velocities with LDA in turbine-agitated tanks with diameters of 0.12, 0.29 and 0.90 m. They suggested a scaling for the mean radial velocity which implies that radial velocity normalized to impeller tip speed is only dependent upon radial position and not on agitation rate or equipment

*Corresponding author. Tel.: +46-46-222-9807; fax: +46-46-222-4622; e-mail: christian.tragardh@livstek.lth.se

Abbreviations: CTA, Constant temperature anemometry; FFT, Fast Fourier transform; HFA, Hot film anemometry; LDA, Laser Doppler anemometry

1385-8947/99/$ – see front matter
PII: S1385-8947(98)00147-8

size. They also found the wave number at the change of the energy spectrum to be inversely proportional to the vessel diameter, but did not scale their spectra with any local flow parameter.

Ogawe [15–17] have presented a suggestion for scaling of the energy spectrum function in a different equipment, based on pipe flow measurements. They proposed a general equation for the energy spectrum function for wide wavenumber ranges, where the spectra were scaled to a mean wave number which was assumed to be proportional to the size of the vessel. Based on the results of Ito [10], they assumed that the fluctuation in the flow was proportional to nd_{imp}. They used the global scale-up rule proposed by Leng [18], where nd_{imp}^{x} is assumed to be constant for reactors of different sizes but similar geometries, and x depends on the type of process. For dispersion processes characterized by turbulent flow, $x = 0.67$. This global rule was replaced by the local characteristic $\overline{u^2}d_{imp}^{-x}$ and the energy spectra were scaled by this expression. Their conclusions were that scale-up is successful if the volume scale-up ratio is less than 27 by keeping the turbulent kinetic energy constant, $\overline{u^2}d_{imp}^{0}$, but when the scale-up ratio is greater than 27, then x depends upon the process. If the higher wavenumbers play a significant role, then $\overline{u^2}d_{imp}^{2/3}$ should be kept constant. If the lower wavenumbers play a significant role then $\overline{u^2}d_{imp}$ is assumed to be constant.

In this paper, results from measurements of turbulent velocities in three different reactors are presented. The pilot-scale is 0.8 m in diameter and equipped with two Rushton turbines. The industrial reactors have diameters of 1.87 and 2.09 m and are equipped with three and four Rushton impellers, respectively. Measurements were conducted with constant temperature anemometry (CTA) with a split-film probe, measuring in two dimensions simultaneously. The local flow parameters, mean velocities, convective velocity, turbulent intensities, turbulent kinetic energy and energy dissipation rate, as well as energy spectra, were calculated from the measurements and scaled with appropriate parameters for each reactor.

2. Materials and methods

Measurements of turbulent velocities were performed in three different reactors equipped with Rushton turbines of standard geometry, $W = d_{imp}/5$ and $L = d_{imp}/4$. The geometry of tank A, B and C is shown in Fig. 1(a), (b) and (c) respectively, and the corresponding data are given in Table 1. Experiments were carried out at the position of the lower impeller in tanks A and B. In tank C, measurements were conducted at the position of the third impeller. In tanks A and C, the measurement positions were on the centreline of the impeller, see Fig. 1(a) and (c). Due to geometric restrictions, the measurement positions in tank B were below the centreline ($2z/W = -0.5$), see Fig. 1(b).

Microfiltrated water was used as liquid and the temperature was kept constant, as required by the measuring method. A plastic lid was used to cover the liquid surface

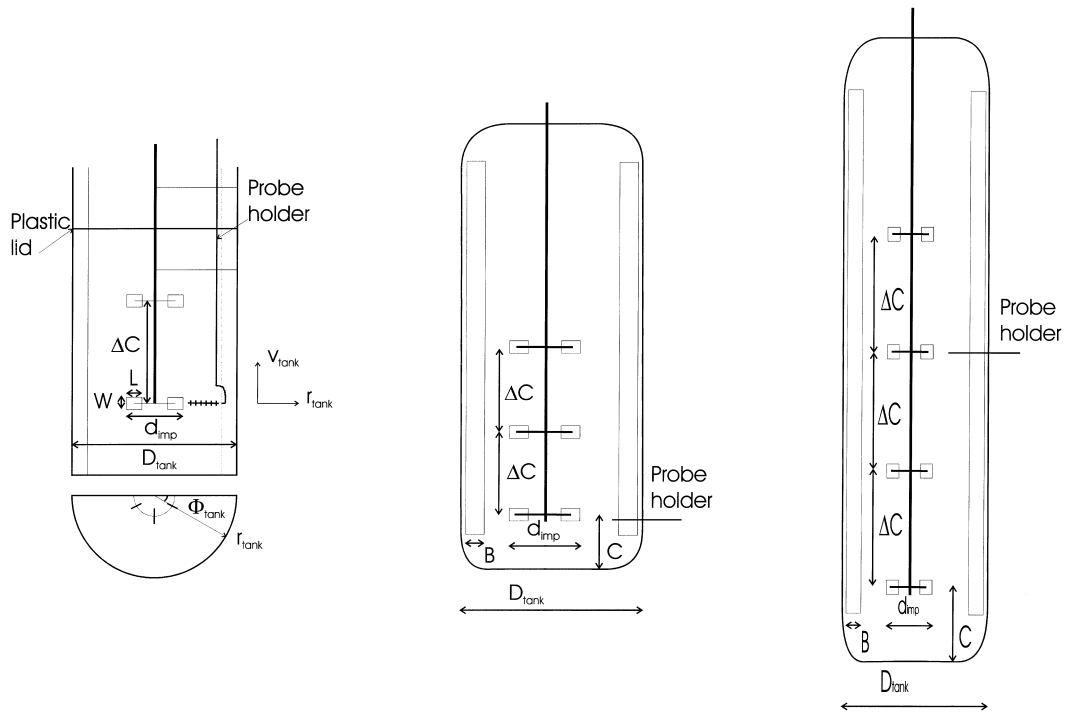

Fig. 1. View of (a) tank A showing probe holder, measuring positions and tank coordinates, (b) Tank B with probe holder position, and (c) Tank C with probe holder position.

Table 1
Configuration data for the three reactors

	Tank A	Tank B	Tank C
Tank diameter, D_{tank} (m)	0.8	1.88	2.09
Tank-to-impeller diameter, D_{tank}/d_{imp}	3	2.47	3
No. of impellers	2	3	4
Bottom clearance, C[a]	0.425	0.3	0.5
Impeller spacing, ΔC[a]	0.7	0.45	0.7
Liquid height, H_v[a]	1.5	2.4	3.5
Liquid volume,V_L (m^3)	0.60	11.7	22
Baffle width, B[a]	0.10	0.10	0.09

[a] Lengths are normalized with tank diameter, D_{tank}.

in tank A to prevent surface aeration and the creation of bubbles in the liquid. In reactors B and C, the liquid depth above the measurement positions of the probe considerably reduced the aeration phenomena. A lid was also used by Nouri in Rutherford [9], where the former have shown that the use of a lid only affects the flow close to the lid/free liquid surface, and the flow velocities were almost identical everywhere else in the vessel.

Turbulent velocities were measured with CTA using a two-channel system (DISA CTA 56C17) and a split-film probe especially designed for water (DANTEC R55). The probe has a measuring length of 1.25 mm and a diameter of 0.200 mm. Instantaneous velocities were measured in two directions simultaneously.

In tank A, the probe was inserted through the lid of the reactor 30° from the baffle, (see Fig. 1(a)). The probe holder was rotated until the split faced the direction of convective flow, which was 45° from the radial tank direction. In tanks B and C, the probe was inserted through the sampling ports in the side of the tank. The baffles were positioned at 45° relative to the probe holder in tanks B and C. The probe was located in the radial/axial (r_{tank}, x_{tank}) plane of the tank, measuring velocities in the radial/tangential (r_{tank}, Φ_{tank}) plane of the tank.

The instantaneous velocities were transformed into flow coordinates according to Fig. 2. Calibration was carried out before and after measurements, using a special calibration

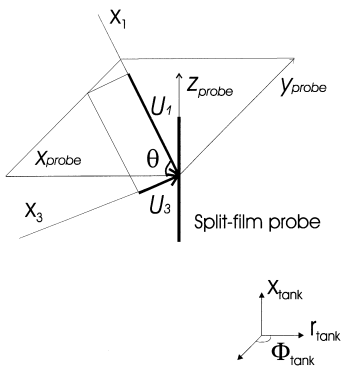

Fig. 2. Coordinate system for the split-film probe measuring in the radial/tangential plane in the tank (x_1 is the convective direction).

Table 2
Sampling times and sampling frequencies

Tank	Sampling time [s]	Sampling frequency [kHz]
A	280	15
A	420	10
B	420	10
C	20	25

unit, to ensure that the measuring system was stable during the measurements. Details concerning calibration are given elsewhere [19].

Voltages from the two-channel system were connected to an A/D converter with a sample-and-hold card, CIO-AD16JR-AT (Computer Boards). Data were collected simultaneously from the two films and stored in compressed form on the host computer, a PC 386. The sampling times and sampling frequencies used are in Table 2.

For the calculation of autocorrelation of velocities, subroutines from the Numerical Recipes for Fortran [20], were implemented in the programs using Fast Fourier Transforms, FFT. The calculations were carried out on an IBM RISC 6000 computer with 80 MB internal memory.

Global parameters which refer to the operating conditions in the tanks are the Reynolds impeller number, Re_{imp}, and the impeller tip speed, v_{tip} (see Eq. (1) and Eq. (2)).

$$\mathrm{Re} = \frac{d_{imp}^2 n}{v} \tag{1}$$

$$v_{tip} = \pi n d_{imp} \tag{2}$$

The operating parameters used for the three reactors are given in Table 3.

2.1. Local scale-up parameters

The local turbulent parameters of main interest for scale-up are the turbulent kinetic energy, q, and the local energy dissipation scale, ε. Turbulent kinetic energy is composed of the mean of the fluctuations of the flow, $\overline{u_i^2}$, in all three directions of flow, (see Eq. (3)). However, in the industrial tanks B and C, the measurements were performed in the radial/axial plane of the tank. Therefore, $\overline{u_2^2}$ was approximated to $\overline{u_3^2}$ as they are close to being equal [19] The same

Table 3
Operating parameters for three tanks of different geometry

	n [s]	Re_{imp} $[-]\cdot 10^{-4}$	v_{tip} $[ms^{-1}]$
Tank A	3.67	24.1	3.07
Tank B	1.08	57.9	2.59
	1.33	71.3	3.18
	1.70	90.9	4.06
Tank C	1.92	87.1	4.22
	2.22	100.6	4.87

approximation was applied for the measurements in tank A, although measurements were performed in all three directions.

$$q = \tfrac{1}{2}(\overline{u_1^2} + \overline{u_2^2} + \overline{u_3^2}) \tag{3}$$

The local energy dissipation was calculated from energy spectra, using Kolmogorov's spectrum law Eq. (4). This states that if the local Reynolds number, Re_λ, is large enough, the local energy dissipation can be estimated from the slope of the energy spectrum, since this part of the spectrum represents the internal subrange of the wavenumbers, and local isotropy exists.

$$E(k) = A\varepsilon^{2/3}k^{-5/3} \quad \mathrm{Re}_\lambda^{3/4} \gg 1 \tag{4}$$

The coefficient A was set to 0.47, as was done by Grant et al. [21] for measurements in a tidal current. Other values: 0.53 for pipe flow, and 0.55 and 0.53 for outer layers and inner layers of shear flow, have been reported in the literature [22].

The mean fluctuations, being the second moment of the probability density function *B(u)*, Eq. (5), can also be expressed as an energy spectrum, *E(f)* Eq. (6), where the amplitudes of the fluctuations are a function of frequency *f*, [23].

$$\sigma_u^2 = (\overline{u_i^2}) = \int_{-\infty}^{\infty} u_i^2 B(u_i)\, du_i \tag{5}$$

$$\overline{u_i^2} = \int E_1(f)\, \mathrm{d}f \tag{6}$$

The energy spectrum can be converted into wavenumber range, through Eqs. (7) and (8), using the convective velocity U_{conv}.

$$k = \frac{2\pi f}{U_{\mathrm{conv}}} \tag{7}$$

$$E_1(k) = \frac{U_{\mathrm{conv}}}{2\pi} E_1(f) \tag{8}$$

The energy dissipation lengths, λ_{f} and λ_{g}, are calculated from the Eulerian time scale, $\tau_{\mathrm{E},i}$, which is estimated from the autocorrelation function, $R_{\mathrm{E},i}$, multiplied by the convective velocity, (see Eqs. (9)–(11)).

$$R_{\mathrm{E},i}(t) = \frac{\overline{u_i(\tau)u_i(\tau - t)}}{u_i^2} \tag{9}$$

$$\frac{1}{\tau_{\mathrm{E}}^2} = -\frac{1}{2}\left[\frac{\partial^2 R_{\mathrm{E},i}}{\partial t}\right] \tag{10}$$

$$\lambda_{\mathrm{f}} = 2\lambda_{\mathrm{g}} = U_{\mathrm{conv}}\tau_{\mathrm{E},i} \tag{11}$$

In most measurements presented in the literature, the convective velocity is reduced to the mean velocity in the local flow situation, based on Taylor's hypothesis [1–3,10,13,14, 5,24,11]. Heskestad [25] proposed an extension of the Taylor hypothesis where the fluctuations were also taken into consideration, resulting in (Eq. (14)). This expression was used by Okamoto [26] et al. (1981) and Wu and Patterson [7], however, Okamoto [26] assumed isotropy *i.e.* $\overline{u_1^2} = \overline{u_2^2} = \overline{u_3^2}$, while Wu and Patterson [7] measured all three directions.

$$U_{\mathrm{conv}}^2 = \overline{U_1^2} + \overline{u_1^2} + 2\overline{u_2^2} + 2\overline{u_3^2} \tag{12}$$

Mean velocities, $\bar{U}_i$ and turbulent intensities, I_i, were normalized to the convective velocities or the tip speed, v_{tip}, as in Eq. (13) and Eq. (14).

$$I_i = \frac{\sqrt{\overline{u_i^2}}}{U_{\mathrm{conv}}} \tag{13}$$

$$I_i = \frac{\sqrt{\overline{u_i^2}}}{v_{\mathrm{tip}}} \tag{14}$$

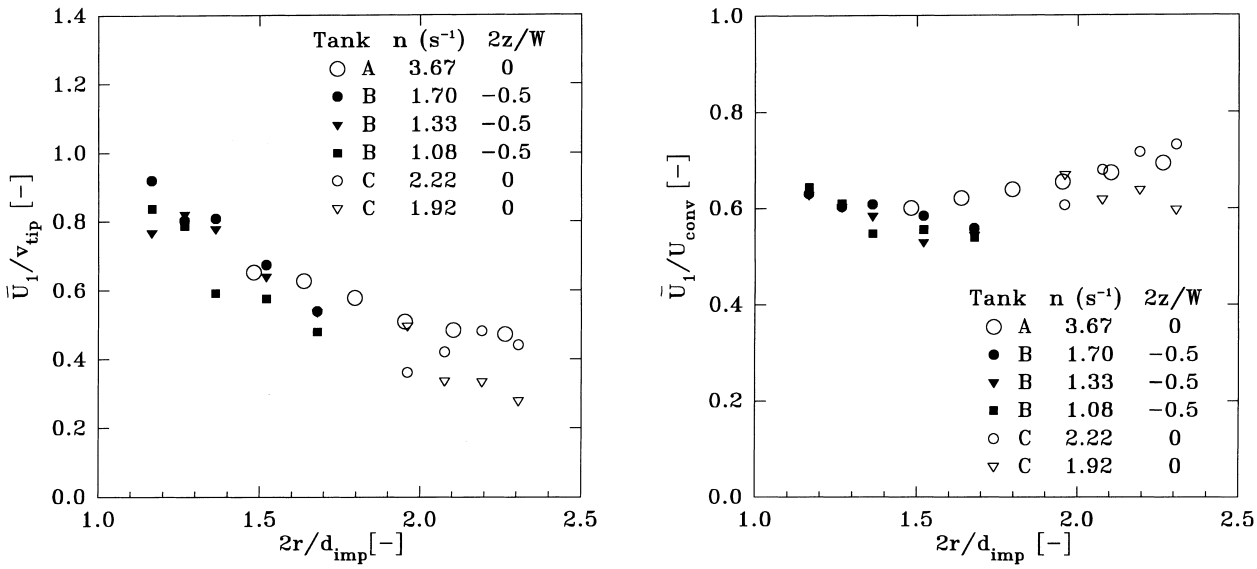

Fig. 3. Mean velocity $\bar{U}_1$ (a) normalized to the tip speed, v_{tip}, in the impeller zone. The dimensionless radial coordinate, $2r/d_{\mathrm{imp}}$, is 1.0 at the impeller tip and 2.4 at the baffle for tanks A and C. For tank B, the coordinate is 1.97 at the baffle, (b) normalized to the convective velocity, U_{conv}, in the impeller zone.

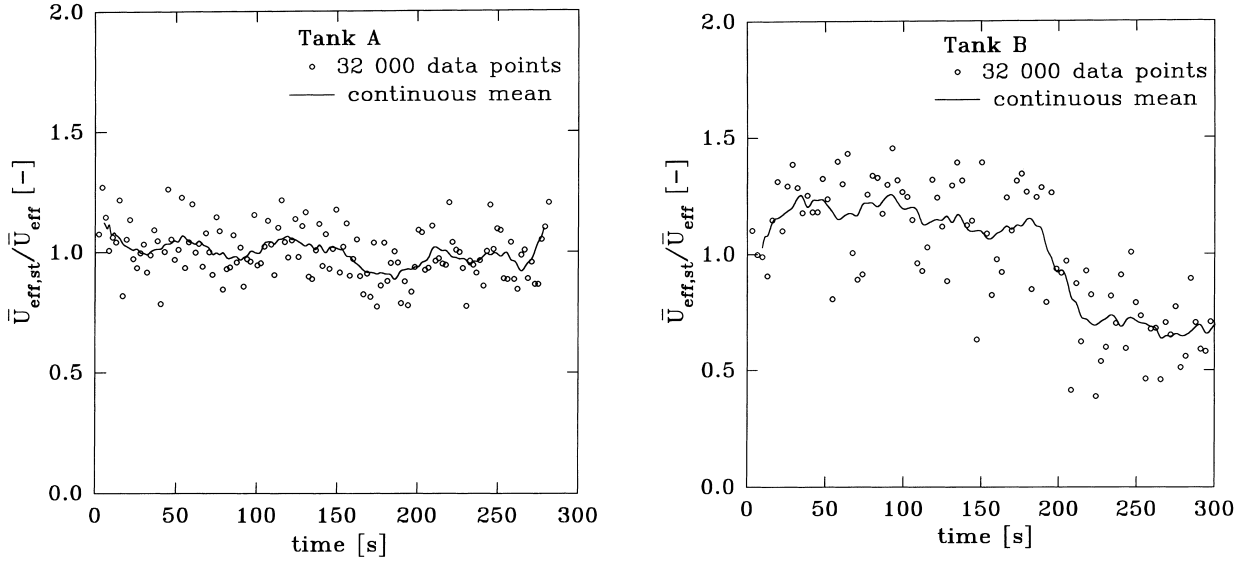

Fig. 4. The variation of short-time averages of the effective velocity, $U_{\mathrm{eff,st}}$ as a function of measuring time in (a) Tank A, (b) Tank B. Notice the long-term variation in the continuous mean value.

3. Results and discussion

In Fig. 3(a), mean velocities $\bar{U}_1$ in the impeller stream, in the convective direction, are shown normalized to the tip speed. The impeller diameter, d_{imp}, was chosen as the scaling length of the radial dimensionless coordinate. As expected, the ratios decrease with radial distance in all three reactors. The ratios in the different positions are dependent on the agitation rate, as shown by the measurements in tanks B and C and presented earlier for tank A [12]. The decrease in the mean velocity as a function of radial position seems to be faster in tank B. This might be due to the measurement position being below the centreline of the impeller. Surprisingly, the values for tank B are in the same range as those of the others, despite the fact that the measurements were made below the centreline of the impeller. The different tank-to-impeller ratios may cause this unexpected similarity. Profiles in the literature show a clear decrease in the mean velocity as a function of the position across the impeller blade [7], see e.g. Wu and Patterson.

Another possible explanation of the larger normalized mean velocities of tank B could be that the impeller spacing is 0.45 compared with 0.7 for the other two reactors. This means that the bulk zone volume is smaller in this reactor than in tanks A and B. It is in the bulk zone that the flow loses its intensity, and if the ratio of this volume to the total volume is lowered, then the flow maintains its turbulent properties to a greater extent.

In Fig. 3(b), the mean velocities $\bar{U}_1$, normalized to the convective velocity, U_{conv}, are shown. This results in a ratio $\bar{U}_1/\bar{U}_{\mathrm{conv}}$ of 0.62 ± 0.05, independent of position. There is, however, a trend for the mean value to decrease slightly with radial position for the measurements in tank B. Here again, the axial coordinate was below the centreline of the impeller, which probably affected the magnitude of the mean velocity. In tank A there is a slight increase in the ratio with radial position. This was also observed in tank C, where the measurement positions were comparable, both for some radial positions and in the axial position ($z = 0$).There is some scatter in the mean velocities of the measurements made in tank C. This might be due to the shorter sampling time in these measurements compared with those for tanks A and B.

The effective velocity, U_{eff}, is the measured resultant velocity of $\bar{U}_1$ and $\bar{U}_3$ and its magnitude is close to the mean velocity in the convective direction, x_1. In Fig. 4(a)

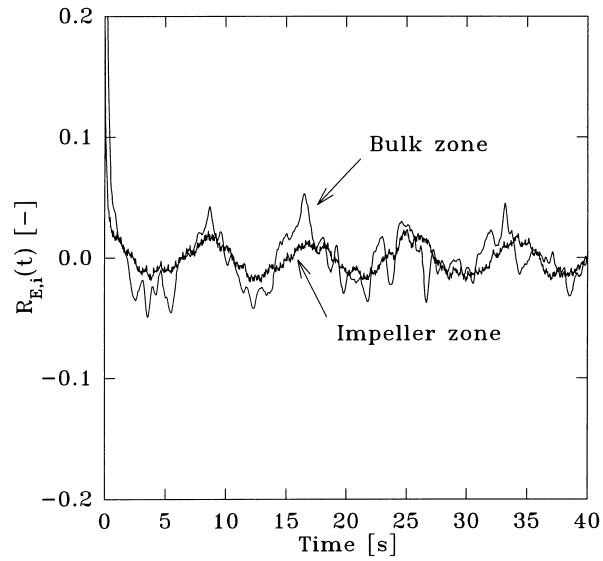

Fig. 5. Autocorrelation for impeller zone and bulk zone for the convective directions.

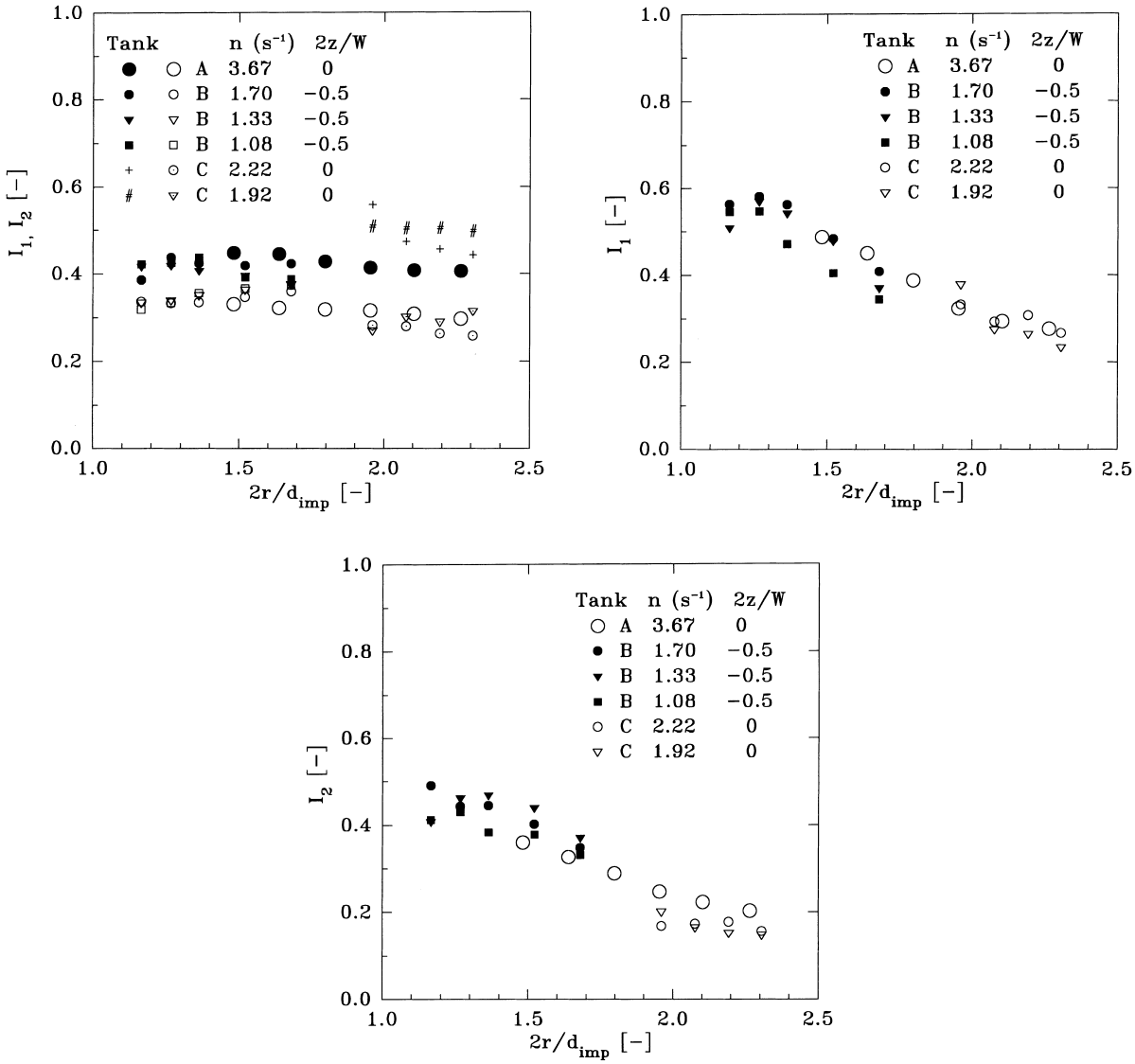

Fig. 6. (a) Turbulent intensities in the convective direction, I_1 (filled symbols) and the perpendicular direction, I_2 (open symbols) . Reference velocity is the convective velocity, U_{conv}, (b) Turbulent intensities in the convective direction, I_1. Reference velocity is the tip speed, v_{tip}, and (c) Turbulent intensities in the perpendicular direction, I_2. Reference velocity is the tip speed, v_{tip}.

and Fig. 4(b), short-time averages of the effective velocity, U_{eff}, are represented by circles, each representing 32 000 data points. The lines represent a continuous mean, over time, of these short-time averages (10 × 32 000 data points). It can be seen in these figures that there appears to be a long-term fluctuation in the effective velocity in tank B. This is not explained by deviations in agitation rate, which was ±2 rpm. This phenomenon is more pronounced for larger reactors and we suggest that it may be caused by interacting large eddies in the bulk zone. Chapple and Kresta [27] examined different reactor geometries with tuft visualisation, and they also found the circulation pattern to have a time-varying nature which as we suggest must have the same origin. The autocorrelation given for two positions under the same conditions and in tank A also supports this hypothesis. It is given in Fig. 5 and suggests a periodic behaviour of the flow.

The intensity, I_i, scaled with the convective velocity, U_{conv}, is almost constant at one level for the convective direction and at a lower level for the perpendicular direction, see Fig. 6(a). In Fig. 6(b) and (c), v_{tip} is used as a reference velocity. The intensity, as expected, decreases with radial position, both in the convective direction and in the perpendicular direction. This is in agreement with previous measurements [7]. The magnitude of the ratios, however, is higher in our measurements. In this study, the contribution from the periodic pseudo-turbulence has not been subtracted as by Wu and Patterson [7], but it is anyhow almost negligible at these radial distances. As for the mean velocity, we also noticed a dependency on agitation rate.

The value of turbulent kinetic energy as a function of radial position are scaled to the square of the impeller tip velocity is shown in Fig. 7(a). Tanks B and C, having approximately equally sized impellers, are compared at

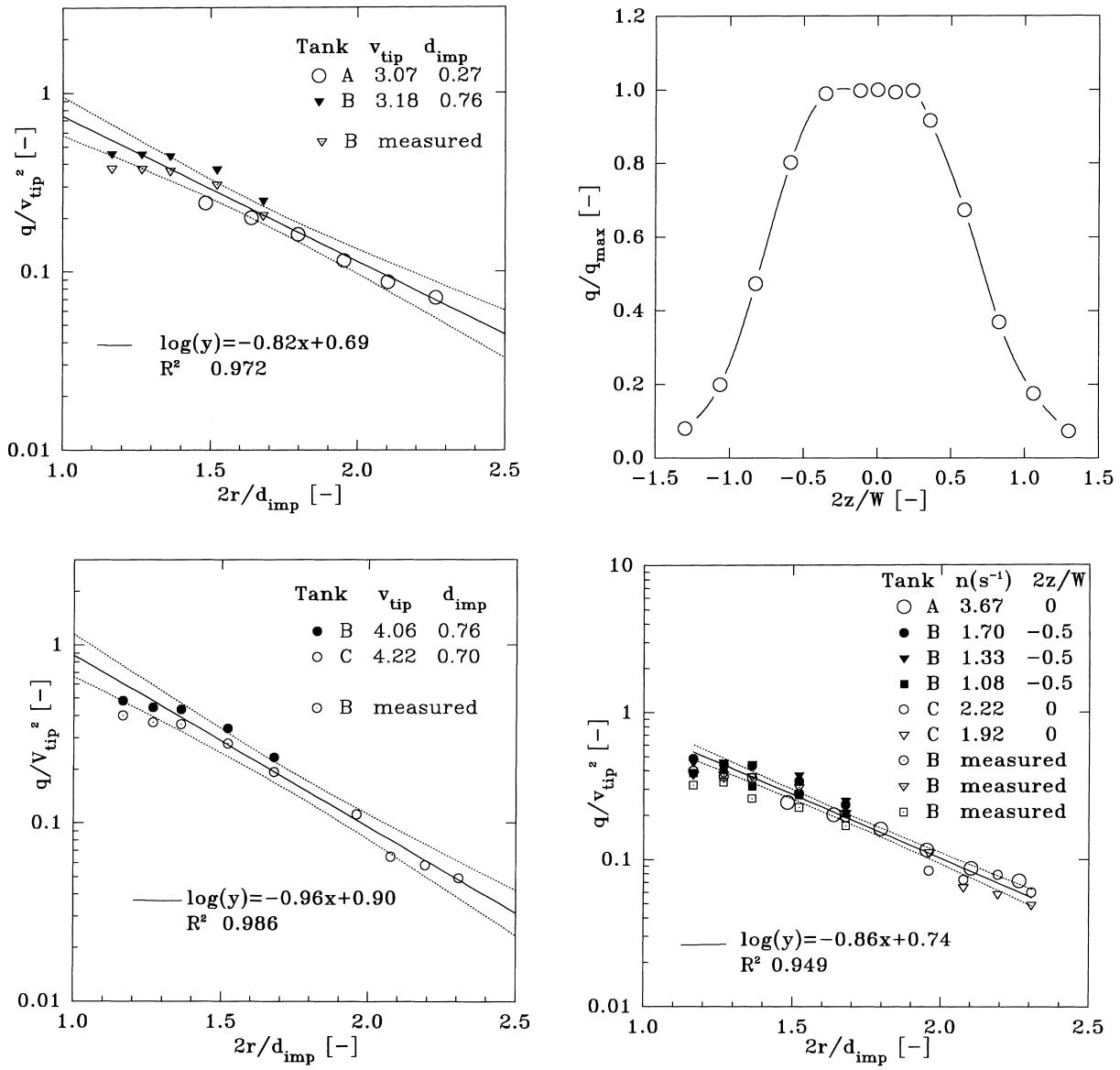

Fig. 7. (a) Comparison of turbulent kinetic energy, q, normalized to the tip speed, v_{tip}, squared in two tanks with similar impeller diameter at *similar* tip speed. The values presented for tank B are adjusted to the magnitude of the expected values at a centreline position, using the profile in Fig. 7 (b) (b) A profile of turbulent kinetic energy, q/q_{max}, over the impeller blade in tank A (c) Comparison of turbulent kinetic energy, q, normalized to the tip speed, v_{tip}, squared in two tanks with different impeller diameter at similar tip speed. The values presented for tank B are adjusted to the magnitude of the expected values at a centreline position, using the profile in Fig. 7 (b) (d) Comparison of turbulent kinetic energy, q, normalized to the tip speed, v_{tip}, squared in three tanks with different impeller diameters and different tip speed. The values presented for tank B are adjusted to the magnitude of the expected values at a centreline position, using the profile in Fig. 7 (b).

similar tip velocities. There is a decrease in the turbulent kinetic velocity, which may be described by a log–linear relationship, according to Eq. (15).

$$\log\left(\frac{q}{v_{tip}^2}\right) = a\left(\frac{2r}{d_{imp}}\right) + F \tag{15}$$

However, the measurements in tank B were performed below the centreline in the impeller stream. A profile of the turbulent kinetic energy, measured across the impeller blade for tank A, is shown in Fig. 7(b). These results indicate that the turbulent kinetic energy at the positions, $2z/W = \pm 0.5$ W, may be approximated to 0.825 q_{max}. Therefore, these values for tank B, comparable to a centreline position, are included in the figure together with the measured data.

In Fig. 7(c), the turbulent kinetic energy measured in tank A is compared with that in tank B. For these two cases, the impeller sizes are different but the tip velocities are similar and the slope of the decrease in the turbulent kinetic energy is similar to the slope in Fig. 7(a). Finally, in Fig. 7(d), the measurements in all three tanks are shown. They result in a

slope similar to those in Fig. 7(a) and Fig. 7(c). These results indicate two things: (1) the agitation rate in these measurements does not affect the magnitude of the normalized value of q significantly, and (2) there is a general decrease in the turbulent kinetic energy as a function of radial position, which can be expressed by (Eq. (15)) for reactors of different sizes. Rutherford [9] measured the turbulent kinetic energy with LDA in tanks with diameters of 0.100 and 0.294 m, with a dual-impeller configuration. They show contour plots of q/v_{tip}^2, where the contours in the impeller zone range over at least one decade, which is comparable to our results. Zhou and Kresta [28] have made LDA measurements of the turbulent kinetic energy in the near impeller region and obtained a non-dimensional energy level of 0.85 which agrees very well with extrapolated data presented here.

The turbulent kinetic energies, normalized to the convective velocity for all three tanks, are shown in Fig. 8. The result of these measurements is a q/U_{conv}^2 ratio of 0.20 ± 0.02. This means that the impeller flow in reactors of different sizes, at different positions and for different operating conditions, can be scaled by a single value. (The values for reactor B have not been adjusted to a centreline position.)

In Fig. 9, the local energy dissipation rates scaled to the convective velocities and the impeller diameters are shown. For this parameter, a constant $\varepsilon d_{imp}/U_{conv}^3$ ratio of 0.32 ± 0.11 is the result of the measurements in the three reactors. The values are somewhat more scattered than those for the turbulent kinetic energy, but the determination of the energy dissipation rate is very sensitive to deviation from ideal theoretical conditions for which it is developed.

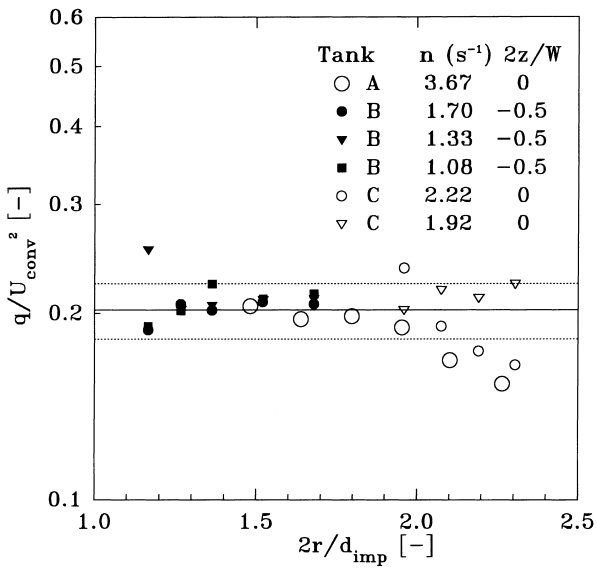

Fig. 8. Turbulent kinetic energy, q, normalized to the convective velocity, U_{conv}, squared for measurements in the impeller zone in the three tanks. Mean ratio $= 0.20 \pm 0.02$.

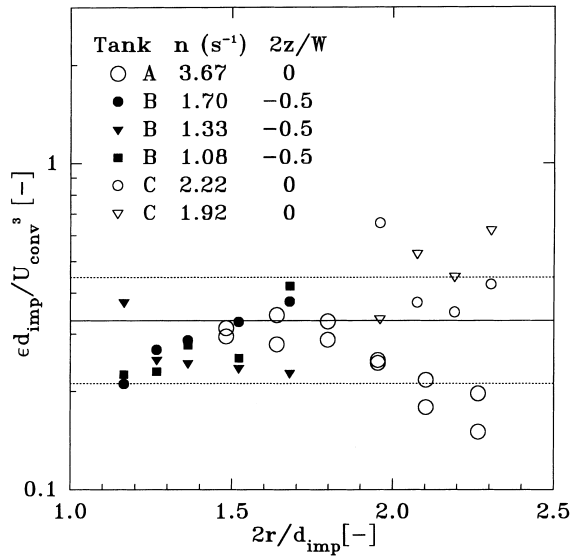

Fig. 9. Local energy dissipation rates and the impeller diameter, εd_{imp}, normalized to the cube of the convective velocity, U_{conv}, for measurements in the impeller zone in the three tanks. Mean ratio $= 0.32 \pm 0.11$.

The values of local energy dissipation rates, scaled to the impeller tip speed and impeller diameter, are shown in Fig. 10. As for the turbulent kinetic energy, the energy dissipation rates are a function of radial position which may be expressed by Eq. (15). The regression coefficients for the measurements in tank A and for the measurements in both tanks A and C are given in the figure. Comparing these results with those of Zhou and Kresta [29], they seem somewhat higher. The non-dimensional energy dissipation rate calculated by Zhou and Kresta is in the range of 0.42 in

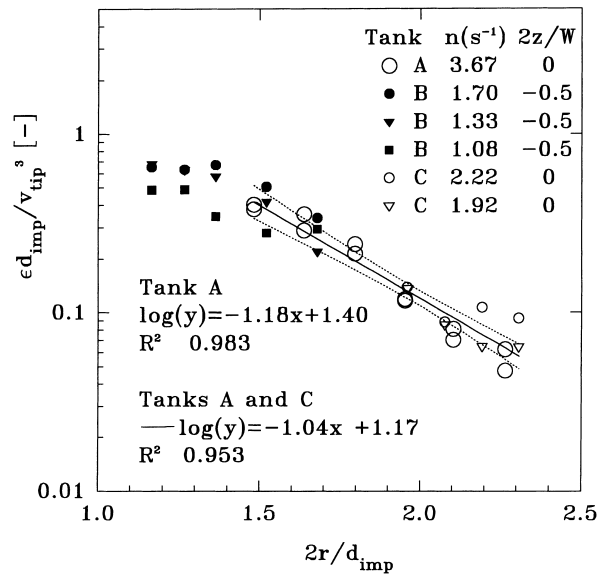

Fig. 10. Local energy dissipation rates and the impeller diameter, εd_{imp}, normalized to the cube of the tip speed, v_{tip}, for measurements in the impeller zone in the three tanks. The local energy dissipation rate is then a function of the radial position.

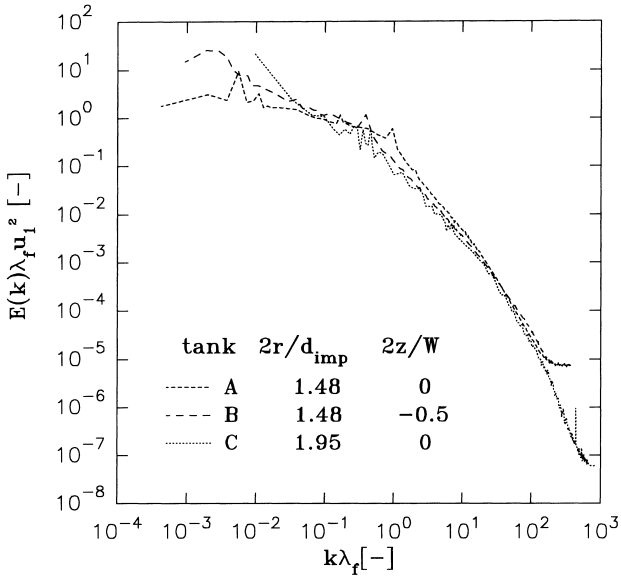

Fig. 11. Energy spectra for the three tanks, in the impeller zone, scaled with the dissipation length λ_f.

the near impeller region and extrapolating these results to the same position yields a value of 0.9. An explanation for this discrepancy can be the different method used. Here, the measurements in tank B are excluded from the slopes, since the measuring point was below the centreline of the impeller.

The hypothesis that the flow characteristics can be reasonably well scaled, independently of the reactor and position, and independently of the agitation rate is also shown in Fig. 11. Here, the spectra from reactors A, B and C are scaled with the local flow parameter, energy dissipation length, λ_f. These spectra overlap, especially in the region of high wavenumbers where the flow becomes isotropic whatever the origin of the convective flow. It is also in this wavenumber region where the major part of the energy dissipation takes place. We have previously shown for reactor A that the spectra overlap when scaled with the energy dissipation length, both in the impeller zone and in the bulk zone [12]. We have also seen that the spectra in the impeller zone for reactor B overlap, regardless of radial position.

This confirms the conclusion by Nishikawa [13], that energy spectra scale with energy dissipation scale. Fig. 11 shows that this scaling is valid not only in tanks with diameters of $0.15 < D_{tank} < 0.60$ m, but also in pilot and industrial sized tanks, $0.8 < D_{tank} < 2.09$ m, and with tanks of different geometries.

4. Conclusions

Turbulent velocity measurements were carried out with CTA in a tank of pilot size and in two industrial tanks. Despite the mechanical constraints that the existing industrial production units implied related to possibilities in doing whatever measurements wherever wanted, it was still possible to obtain satisfactory data in view of the objectives of the work.

The convective velocity is a scaling parameter of the flow. Using v_{tip} as a scaling parameter relates the measured parameters to the geometry of the system. The turbulent quantities, q and ε, can approximately be estimated in the impeller zone, for reactors over a large range of sizes and different geometries under relevant operating conditions from the data presented.

The ratio of bulk zone volume to impeller zone volume influences the convective and the turbulent flow pattern in the impeller zone. The convective flow is probably affected by interacting large eddies in the bulk zone, resulting in time-varying characteristics of the mean flow. The turbulent part of the flow is seen to remain high in intensity.

The energy spectra show that the flow has an isotropic character in the high wavenumber range, where the slope is proportional to $k^{-5/3}$, according to Kolmogorov's law of local isotropy. It can also be seen that the flow has a long-term periodic fluctuation character, shown by the shape of the autocorrelation function, the behaviour of the short-time averages of the effective velocity, combined with the large amplitude of the energy spectra in the low wavenumber region. This is more pronounced in the larger industrial tank.

In the impeller zone, neither the size of the tank nor the differences in geometry influenced the flow parameters when they were scaled by local flow parameters. On the other hand, the magnitudes of the turbulence parameters are determined by the size of the tank and the impeller.

5. Notation

A	(–)	coefficient
a	(–)	coefficient
B	(m)	baffle width
$B(u)$	(–)	probability density function, PDP
C	(m)	bottom clearance
ΔC	(m)	impeller spacing
d_{imp}	(m)	impeller diameter
D_{tank}	(m)	tank diameter
$E_1(f)$	($m^2\ s^{-2}$)	one-dimensional frequency spectrum
$E_1(k)$	($m^3\ s^{-3}$)	one-dimensional wavenumber spectrum
f	(s^{-1})	frequency
F	(–)	factor
H_v	(–)	liquid height compared with tank diameter
I_i	(–)	turbulence intensity
k	(m^{-1})	wavenumber
L	(m)	length of the impeller blade
l_K	(m)	Kolmogorov's length scale

n	(s^{-1})	agitation rate
nd_{imp}	($m\ s^{-1}$)	modified tip velocity
q	($m^2\ s^{-2}$)	turbulent kinetic energy
q_{max}	($m^2\ s^{-2}$)	maximum turbulent kinetic energy
r_{tank}, x_{tank}, Φ_{tank}	(–)	radial, axial and tangential tank coordinates
$R_{E,i}$	(–)	autocorrelation function
Re_{imp}	(–)	Reynolds number for impeller
Re_λ	(–)	Reynolds number for energy dissipation scale
t	(s)	time
$\bar{U}_i$	($m\ s^{-1}$)	ensemble time average of mean velocity $i = 1,2,3$
$\bar{U}_{conv}$	($m\ s^{-1}$)	convective velocity
$\bar{U}_{eff}$	($m\ s^{-1}$)	effective velocity, $(U_1(t)^2 + U_2(t)^2)^{1/2}$
$\bar{U}_{eff}$	($m\ s^{-1}$)	ensemble time average of U_{eff}
$\bar{U}_{eff,st}$	($m\ s^{-1}$)	short-time average of U_{eff}
x_{probe}, y_{probe} z_{probe}	(–)	probe coordinates
$\overline{u_i^2}$	($m^2\ s^{-2}$)	ensemble average of velocity fluctuations, $i = 1,2,3$
v_{tip}	($m\ s^{-1}$)	impeller tip velocity
V_L	(m^3)	liquid volume
W	(m)	blade width
x	(–)	factor
z	(–)	axial coordinate across impeller blade, $z = 0$ at the centre of the blade

Greek letters

ε	($m^2\ s^{-3}$)	energy dissipation rate
λ_f, λ_g	(m)	energy dissipation length scales, Taylor's microscale
τ_E	(s)	Eulerian time scale
θ	(°)	angle for calibration
ν	($m^2\ s^{-1}$)	kinematic viscosity
σ_u^2	(–)	variance

Acknowledgements

This work is part of two projects, Bioreactor Performance within the Nordic Bioprocess Engineering Programme under auspices of NI the Nordic Fund for Technology and Industrial Development and the Bioprocess Technology Programme funded by the Swedish National Board for Industrial and Technical Development, NUTEK. Their support is gratefully acknowledged. This investigation was made possible by the help of Pharmacia and Upjohn, Sweden and Statoil Biosentrum in Stavanger, Norway, who both made their production units available to us. We would also like to thank Scaba AB, Sweden, who supplied the agitation system and the Rushton turbines for tank A.

References

[1] L.A. Cutter, Flow and turbulence in a stirred tank, AIChE J. 12 (1966) 35–45.
[2] M.A. Rao, R.S. Brodkey, Continuous flow stirred tank turbulence parameters in the impeller stream, Chem. Eng. Sci. 27 (1972) 137–156.
[3] I. Komasawa, R. Kuboi, T. Otake, Fluid and particle motion in turbulent dispersion-I. Measurement of turbulence of liquid by continual pursuit of tracer particle motion, Chem. Eng. Sci. 29 (1974) 641–650.
[4] S. Yuu, T. Oda, Measurement of turbulence parameters in a non-baffled stirred tank with high rotation speeds, Chem. Eng. J. 20 (1980) 35–42.
[5] H.D. Laufhütte, A. Mersmann, Dissipation of power in stirred vessels, Paper no. 33, 5th Eur. Conf. on Mixing, Würtzburg, 1985, 331–340.
[6] M. Mahoust, G. Cognet, R. David, Two component LDV measurements in a stirred tank, AIChE J. 35 (1989) 1770–1778.
[7] H. Wu, G.K. Patterson, Laser Doppler measurements of turbulent flow parameters in a stirred mixer, Chem. Eng. Sci. 44(1989) (1989) 2207–2221.
[8] C.M. Stoots, R.V. Calabrese, Mean velocity field relative to a Rushton turbine blade, AIChE J. 41 (1995) 1–11.
[9] K. Rutherford, K.C. Lee, S.M.S. Mahmoudi, M. Yianneskis, Hydrodynamic characteristics of dual Rushton impeller stirred vessels, AIChE J. 42 (1996) 332–346.
[10] S. Ito, K. Ogawa, N. Yoshida, Turbulence in impeller stream in a stirred vessel, J. Chem. Eng. Japan 8 (1975) 206–209.
[11] J. Costes, J.P. Couderc, Study by laser doppler anemometry of the turbulent flow induced by a Rushton turbine in a stirred tank: Influence of the size of the units I. Mean flow and turbulence, Chem. Eng. Sci 43 (1988) 2751–2764.
[12] E. Ståhl Wernersson, Ch. Trägårdh, Scaling of turbulence characteristics in a turbine-agitated tank in relation to agitator rate, Chem. Eng. J. 70 (1998) 37–45.
[13] M. Nishikawa, Y. Okamoto, K. Hashimato, S. Nagata, Turbulence energy spectra in baffled mixing vessels, J. Chem. Eng. Japan 9 (1976) 489–494.
[14] K. Van der Molen, H.R.E. van Maanen, Laser-Doppler measurements of the turbulent flow in stirred vessels to establish scaling rules, Chem. Eng. Sci. 33 (1978) 1161–1168.
[15] K. Ogawe, C. Kuroda, S. Yoshikawa, An expression of energy spectrum function for wide wavenumber ranges, J. Chem. Eng. Japan 18 (1985) 544–549.
[16] K. Ogawe, C. Kuroda, S. Yoshikawa, A method of scaling up equipment from the viewpoint of energy spectrum function, J. Chem. Eng. Japan 19 (1986) 345–347.
[17] K. Ogawe, C. Kuroda, A new scale-up rule and evaluation of traditional rules from a viewpoint of energy spectrum function, in: G.B. Tatterson (Ed.), AIChE Symposium Series, Industrial Mixing Fundamentals with Application, no. 305, 1995, 95–101.
[18] D.E. Leng, Succeed at Scale Up, Chem. Eng. Progress, June 1991, pp. 23–31.
[19] E. Ståhl Wernersson, Ch. Trägårdh, Measuring and analysis of high-intensity turbulent characteristics in a turbine-agitated tank, to be published in Experiments in Fluids, (1998).
[20] H.L. Grant, R.W. Stewart, A. Moilliet, J. Fluid Mech. 12 (1962) 241–263.
[21] C.J. Lawn, The determination of the rate of dissipation in turbulent pipe flow, J. Fluid Mech. 48 (1971) 477–505.
[22] W.H. Press, S.A. Teukolsky, W.T. Vetterling, B.P. Flannery, Numerical Recipes in Fortran, 2nd ed., Cambridge, 1992.
[23] J. Hintze, Turbulence, 2nd ed., McGraw Hill, New York, 1975.
[24] H.D. Laufhütte, A. Mersmann, Local energy dissipation in agitated turbulent fluids and its significance for the design of stirring equipment, Chem. Eng. Technol. 10 (1987) 56–63.

[25] G. Heskestad, A generalized Taylor hypothesis with application for high Reynolds number turbulent shear flows, J. Appl. Mech. 32 (1965) 735–739.
[26] Y. Okamoto, M. Nishikawa, K. Hashimoto, Energy dissipation rated distribution in mixing vessels and its effects on liquid–liquid dispersion and solid–liquid mass transfer, Int. Chem. Eng. 21 (1981) 88–94.
[27] D. Chapple, S. Kresta, The effect of geometry on the stability of flow patterns in stirred tanks, Chem. Eng. Sci 49 (1994) 3651–3660.
[28] G. Zhou, S.M. Kresta, Distribution of energy between convective and turbulent flow for three frequently used impellers, Trans. IChemE, Part A 74 (1996) 379–389.
[29] G. Zhou, S.M. Kresta, Impact of tank geometry on the maximum turbulence energy dissipation rate for impellers, AIChE J. 42 (1996) 2476–2490.